Journal of Materials and Engineering Structures

Research Paper

FEM analysis of the three dimensional effect of microvoids on the PMMA behaviour in PTH.

Leila Zouambi [a], ***Noureddine Mahmoudi*** [a,*], ***Mokhtar Bourdim*** [a], ***Boualem Serier*** [b]

[a] *Laboratoire Génie Industriel et Développement Durable, Mechanical Engineering Department, University Center Ahmed Zabana of Relizane, Bourmadia, 48000, Algeria.*

[b] *LMPM Mechanical Engineering Department, Faculty of Technology, University of Sidi Bel-Abbes, 22000, Algeria.*

ARTICLE INFO

Article history :

Received : 29 October 2017

Revised : 3 February 2018

Accepted : 3 February 2018

Keywords:

Microvoid

Interface

Stress

Interdistance

ABSTRACT

The performance and success of cemented total hip arthroplasty is related to the stress fields in the cement mantle due to the loading caused by patient activities. To do this, a three dimensional linear elastic model was developed to investigate the intensity and distribution of equivalent stress in the bone cement (PMMA) between the microvoids. This analysis is made according to several parameters such as the size of the microvoids defects, its direction of the arrangement, its location in the seat of the stress concentration and a dependency between limit stress value (in certain stress state) and the third invariant.

1 Introduction

The durability of a total hip replacement depends on the mechanical behaviour of each prosthesis component, especially the surgical cement. Until today the PMMA is the only material used to anchor the femoral implant in to the femoral bone during a cemented arthroplasty. In the cemented hip replacement, the cement is the most fragile material, which has two interfaces; one with the bone and the second with the prosthesis, this cement mantle is the weakest link in the load transfer system (implant – cement – bone) [1]. In general, three types of defects can exist in cement: porosities, inclusions and cracks [2]. The presence of cavities in the bone cement has a great importance for the transport of antibiotics, but its existence in this material can lead to its weakening by notch effect [3]. Several studies have analysed the porosities effect in the cement on its mechanical behaviour; [4] analysed by FEM the behaviour of cracks emanating

* *Corresponding author. Tel.: +213 561557999*
E-mail address: mahmoudi.noureddine@yahoo.fr

e-ISSN: 2170-127X,

RESEARCH REVIEW of Sciences and Technologies

from microvoids according to the patient's activity, localization of porosity, orientation of the cracks and the crack-microvoid and crack-crack interactions by computing the stress intensity factor. [3, 5] analysed by FEM, the size influence of micro-cavities in cement assuming the junction cup-bone, and the effect of cavity-cavity interaction on the stress level and distribution in cement according to the human stance defined by the implant position axis compared to that of the cup.

The mechanical behaviour of total hip prosthesis is, until now, under investigations. This study comes within this context as objective of a three-dimensional analysis of the mechanical behaviour of surgical cement (PMMA) during the patient's daily activities by the finite elements method. This behaviour depends on that of microvoids. These last due to mixing method supposed pre-existing in the site of stress concentration in the orthopaedic cement to predict the risk of fracture. For this purpose, we calculated the normal, shear and equivalent stresses around the microvoids located in area of the cement under static loading. Using the ABAQUS calculation code version 6.11 [6], this study made for different distribution and microvoids localization. The results obtained can help surgeons predict whether early PTH loosening may occur under such conditions.

2 Finite element modelling

The numerical solution using the finite element method is most suited to mechanical problems. Our study was performed using the computer code ABAQUS finite element version 6.11 [7]. The basic structure is three-dimensional. In this study, the elementary three-dimensional model is composed of the cortical bone of the iliac outer layer with a constant thickness of 0.9mm [8]. The trabecular bone was merged into the cortical bone. A polyethylene cup with an internal diameter was 28mm and external diameter of 54 mm was secured by PMMA into an acetabulum with a diameter of 56mm. The thickness of cement bone was 2mm [9]. Fig. 1d present the geometrical model of the reconstructed acetabulum.

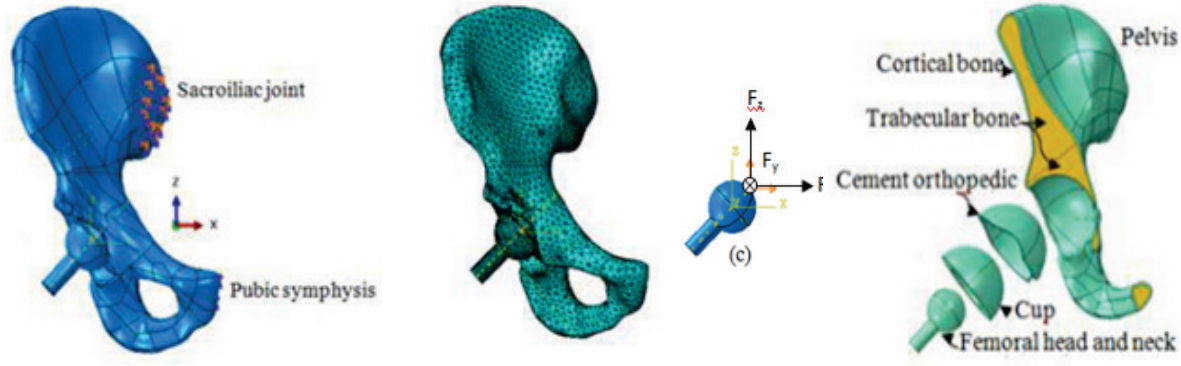

(a) (b) (d)

Fig. 1- Reconstructed acetabulum components
(a) Boundary conditions, (b) Meshed model, (c) Illustration of directions of force components applied to the femoral head (Fx, Fy, Fz), (d) Antero-posterior view of the pelvis and acetabular component.

The commercially available total hip acetabular components, which consisted of a titanium alloys femoral head, a polyethylene acetabular cup and acrylic cement due to their wonderful biocompatibility behaviour in clinical conditions. All the materials were assumed linearly isotropic and homogeneous. This is a reasonable assumption since the stresses are not enough high to create a plastic deformation of the polyethylene. Table 1 gives the elastic properties of the five materials: of prosthetic femoral head, cup, cement, cortical and trabecular bone.

Table 1-Material properties [4]

Materials	**Young's Modulus (MPa)**	**Poisson's ratio (ν)**
Cortical bone	17000	0.3
Cancellous bone	1 to 132	0.2
Subchondral bone	2 000	0.3
PMMA	2 300	0.3
UHMWPE	690	0.3
Femoral head (Titanium alloy)	210 000	0.3

It is known that in general, cement do not resist well to tensile loading. The tensile strength of the cement is 25MPa, the compressive strength is 80MPa and the shearing strength is 40MPa [10].

Computational methods such as finite element method are widely accepted in orthopaedic biomechanics as an important tool used to design and analysis the mechanical behaviour of prosthesis [11]. Three-dimensional finite element model of reconstructed acetabulum was developed from the commercial FE code ABAQUS of a right pelvic bone. The elements of 4-node tetrahedron are used to mesh the structure. In total, there were 23541 nodes and 110919 linear tetrahedral elements of type C3D4 in the mesh models without cavities and 28801 nodes and 132390 elements with cavity: see Fig. 1b. A special mesh refinement is used around the cavity with the aim of increasing the precision of calculations.

The hip contact force with the amplitude F is applied to the centre of the femoral head: see Fig. 1a. The three force components medial (Fx)-ventral (Fy)-proximal (Fz) are reported in the x, y, z coordinate system, which is defined relative to a right-sided femur (Fig. 1c). It is transmitted from the femoral head to the cement across the acetabular cup. The z-axis is the idealized straight midline of the femur; x is perpendicular to z and parallel to the transverse plane, the y-axis points in the Antero-posterior direction. The static load is used for a patient with average body as:

Table 2- The external forces exerted on the PTH system [12].

Force applied to PTH head (N)	F (x)	F (y)	F (z)
702 N	156.67N	96.41N	677.9N

Nodes at the sacroiliac joint and the pubic symphysis were fixed in all degrees of freedom as the boundary condition [8, 12]. The contacts bone/cement and cement/cup were fully tied. That of femoral head (metal)/cup (UHMWPE) having a friction coefficient of 0.25 [13]. This contact was assumed tangential and normal behaviour.

3 Results and discussion

The performance and success of cemented total hip arthroplasty is related to the stress fields in the cement mantle stress due to the loading caused by patient activities. The aim of this study is to analyse, by the finite element method, the level and distribution of equivalent stress in the bone cement based on the inter-distance and location of the microvoids. To illustrate this effect, the distribution and the intensity of the stress generated in perfect and porous cement are analysed.

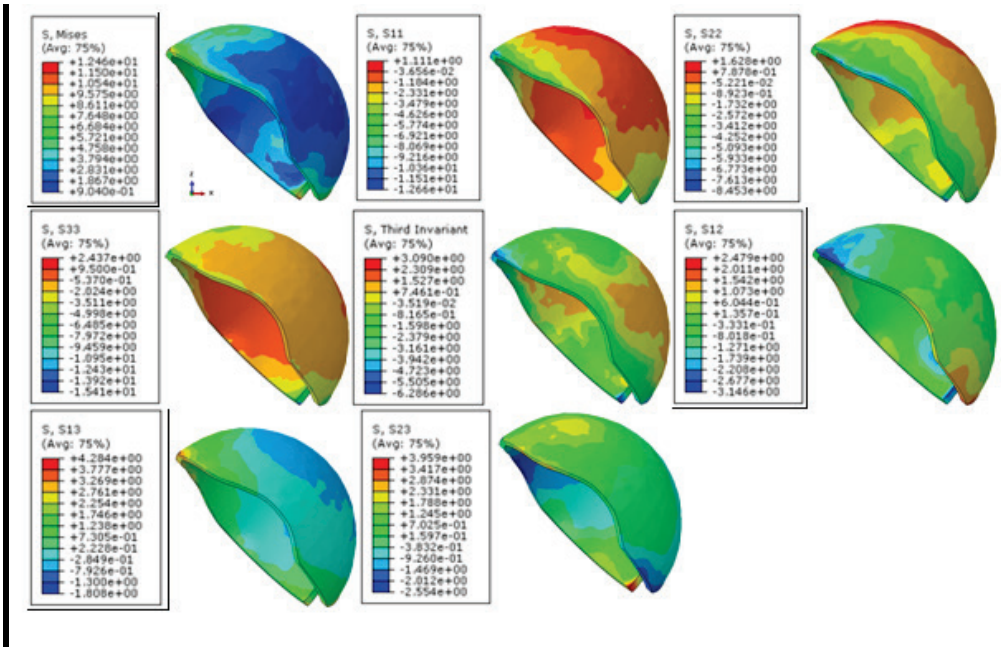

Fig. 2 -distribution of normal, shear and equivalent Stresses in the perfect cement

The figure 2 shows that the stress Induced in the compact cement is more intense near the edge and at the interface with the bone [14]. The results clearly illustrates that the stress distribution is non-homogeneous. These stresses are located

in the free edge of the cement, which is solicited strongly and mechanically. This part of the structure is a seat of the stress concentration. We have assumed the existence of microvoids (with a diameter D=100µm) in this zone due to the process of mixing the cement during its implementation. Such localization allows analysing its effect on the mechanical behaviour of the bone cement.

3.1 Effect of the existence of the microvoids on the mechanical behaviour of the orthopaedic cement

The direct contact between cup-cement-bone in the two extremities of the orthopaedic cement was created in order to know the mechanical responses of the weakest link of the loads transfer chain when the surgeon reaches the acetabulum cavity zone when preparing the implant housing.

In this context, we analysed the distribution of defects (microvoids) located in the most mechanically stressed zone of the bone cement. The inter-distance between the microvoids was assumed 20 µm [5].

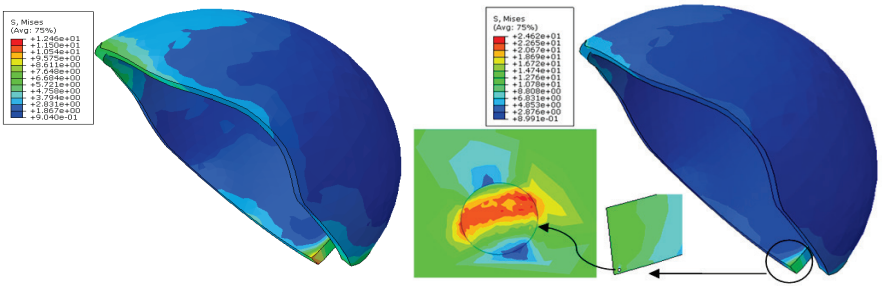

(a) Cement with one microvoid

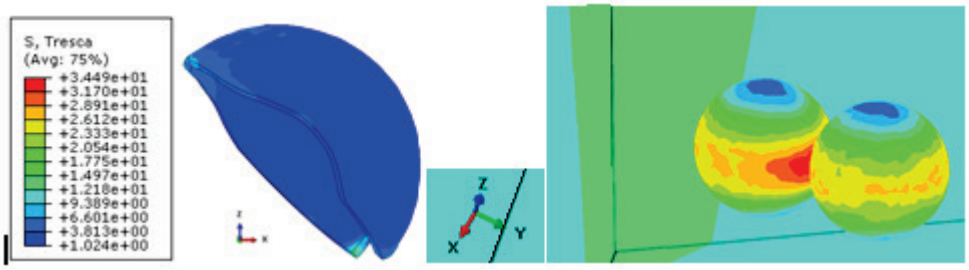

(b) Cement with two microvoids

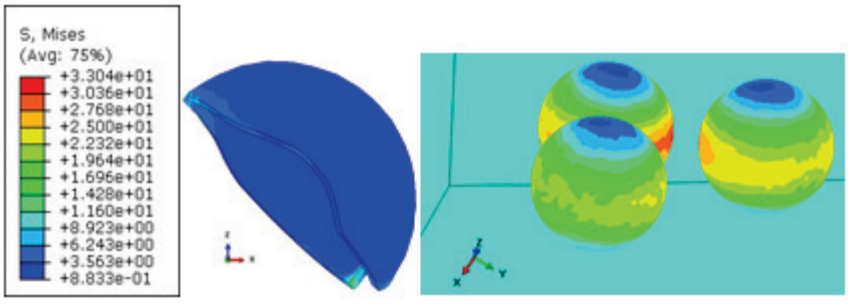

(c) Cement with three microvoids

Fig. 3- Equivalent stress distribution in the cement and around microvoids

The bone cement's response to loading [12] is illustrated in Figure 3. It shows that these stresses are distributed inhomogeneously all over the structure. The equivalent stress of Von Mises is, intensively localized around the microvoids located at the free side of the bone cement and at the interface cement/bone (Fig. 3a). This stress increases as a function of the volume fraction of the microvoids (Fig. 3b & 3c).

3.2 Effect of the distribution of the microvoids:

In this part, we studied the influence of the intensity and distribution of normal, tangential and the equivalent stresses induced in the bone cement (normal stress σ_{zz} and the tangential or shear stress τ_{xz} are represented respectively by σ_{zz} and τ_{xz}) generate from the distribution of localized microvoids in the site of high concentration of stresses. Where the (ox) axis is the lateral axis, the second axis is (oy), and it is the frontal one and the (oz) axis is the vertical one and it is the third axis.

3.2.1 Microvoids aligned in the left of the free side of the cement

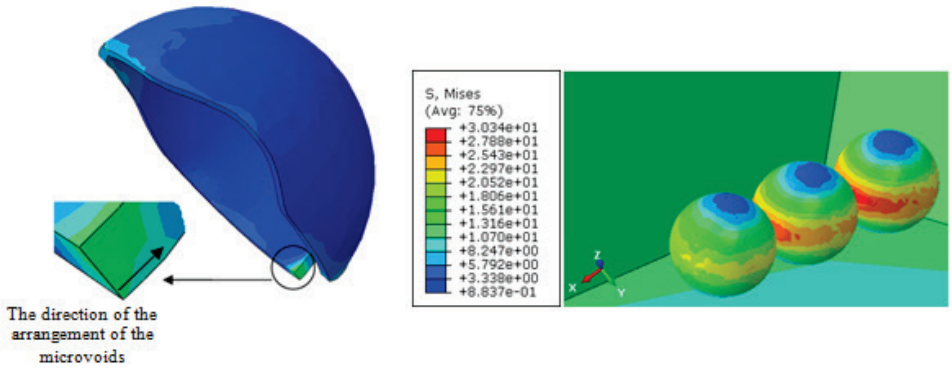

Fig. 4a - Distribution of the equivalent stress of Von Mises; case of aligned microvoids in the left

Fig. 4a illustrates the level and distribution of the equivalent stress induced in the cement and around the aligned cavities as shown in the figure. The highest stresses are located on both sides of the microvoid of the middle, facing the others, distant of 20 µm.

The most significant normal stresses are oriented according to the (oz) axis direction. In fact, the PMMA is subjected to both tensile and compression stress. This is due to the F_z (forces applied according to (oz) direction) acting on the femoral head, will generate an intensively compression stress σ_{33} around the microcavity witch is in the middle. Fig. 4b shows that the resulted compression stress is 25,55MPa while the shear stress magnitude is 16.24MPa. The normal stresses σ_{11} and σ_{22} have opposite intensity magnitudes and are lower level than σ_{33}.

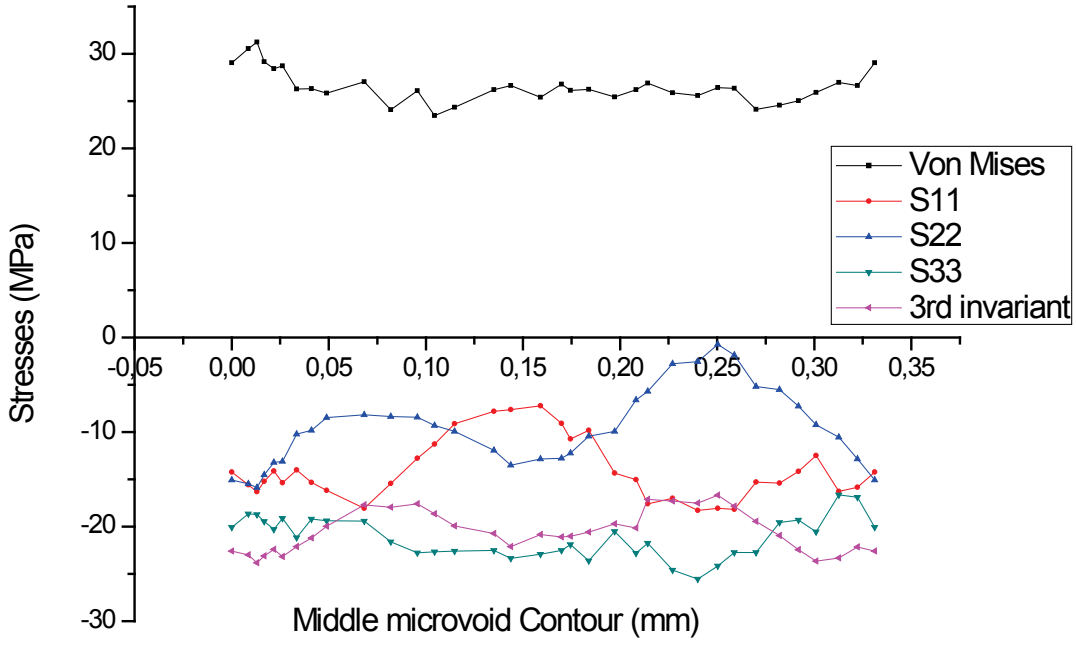

Fig. 4b - Variation of the equivalent, normal and third invariant stresses; case of aligned microvoids in the left

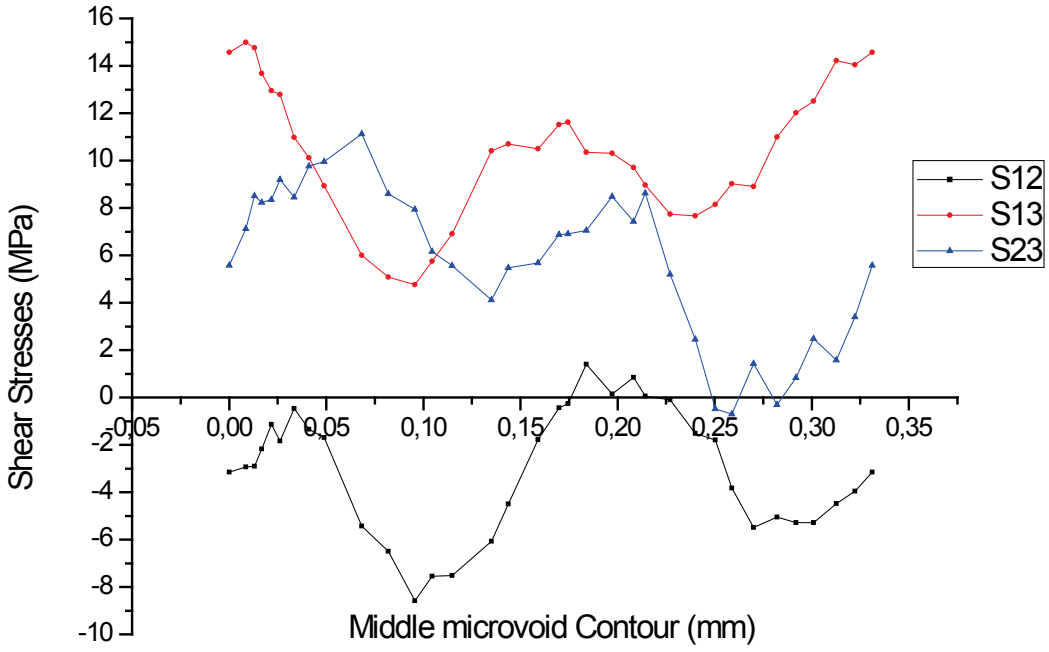

Fig. 4c - Variation of shear stresses; case of aligned microvoids in the left

Stress invariants

It is observed that for certain materials a dependency between limit stress value (in certain stress state) and the third invariant is clearly visible - eg. rocks or certain alloys. As any stress state can be decomposed into a sum of isotropic tensor (hydrostatic pressure) and deviatoric (traceless) tensor, this stress state as a whole can be described in terms of three invariants - first invariant of the stress state (J1) and two invariants of its deviator (J2, J3). J2 describes something that could be named "magnitude" of deviatoric (shearing) stress, while J3 describes the mode of shearing - for pure shears J3=0. Other values of J3 describe various combinations of two or more pure shears (except for two pure shears in mutually perpendicular directions, which reduce to a pure shear itself). It is convenient to formulate limit state conditions for isotropic solids in terms of those invariants. Most of classical limit state conditions (Huber-Mises, Drucker-Prager, Schelicher-Mises, Burzyński, etc.) do not account for the influence of J3 [14].

The material is assumed to be isotropic; hence, the yield surface can be expressed as a function of three invariant measures of the stress tensor: the equivalent pressure stress,

$$p = -\frac{1}{3} trace(\sigma) \tag{1}$$

The yield stress surface makes use of two invariants, defined as the equivalent pressure stress, and the Mises equivalent stress,

$$q = \sqrt{\frac{3}{2}(S:S)} \tag{2}$$

where S is the stress deviator, defined as

$$S = \sigma + pI \tag{3}$$

In addition, the linear model also uses the third invariant of deviatoric stress,

$$r = \left(\frac{9}{2} S.S:S\right)^{\frac{1}{3}} \tag{4}$$

σ is the Cauchy stress tensor, and **I** is the second-order identity tensor [15].

In consequence, in the variations of the third invariant stress around of the middle microcavity illustrated in Fig. 6b, the stress has almost the same appearance but with a minor different in the amplitude variation with the compression stress σ_{33}.

The most important shear stresses are related to (oxz) plane (Fig. 6c) and they are practically localized in the vicinity close to the free edge of the cement and at the cement/bone interface. However, the direct interaction between bone and cement has affected the stresses level in the contact regions but the highest amplitude of shear stresses is much lower than the ultimate shear stresses. The rest of the surgical cement is under low stress intensity.

3.2.2 Microvoids condensed in the free side of the cement

Fig. 7a shows the distribution of the equivalent stress in the case of condensed microvoids. This distribution generates the strongest equivalent stress around the microvoid witch is in the middle. This is explained by the localization of this pore in the vicinity very close not only to the free edge of the cement, which is a geometrical defect but also to the two microvoids. This accentuated the stresses around this defect compared to the previous distribution. Far from this area, the intensity of equivalent stress drops considerably.

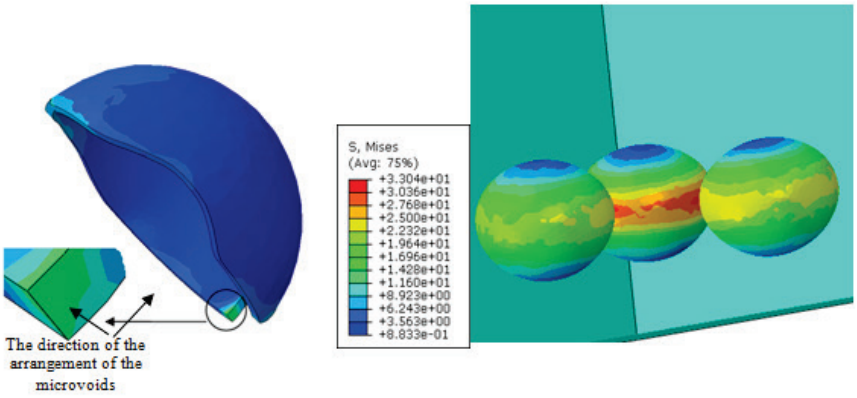

Fig. 5a -Distribution of the equivalent stress of Von Mises; case of condensed microvoids

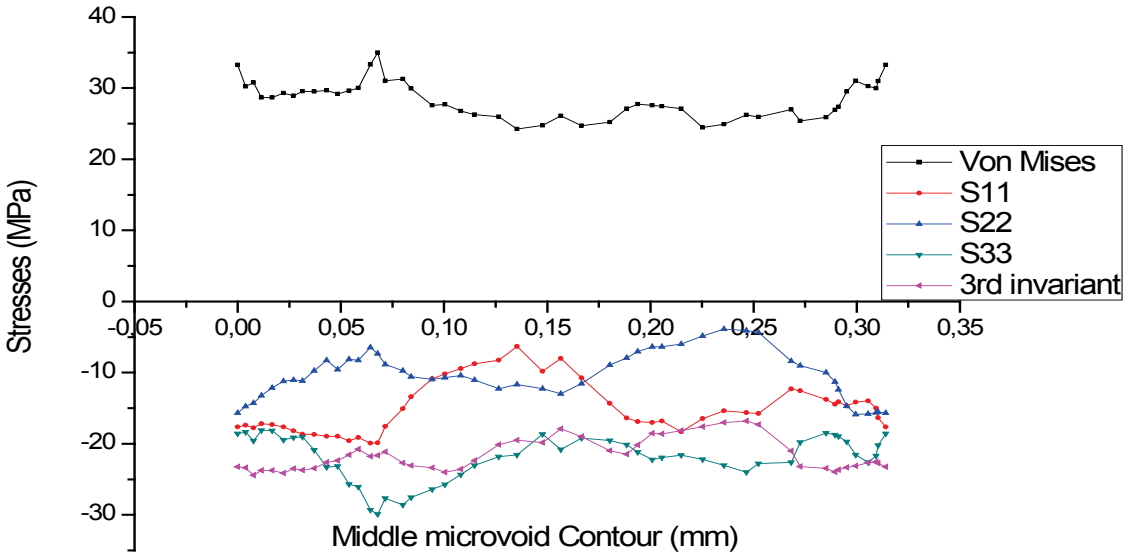

Fig. 5b -Variation of the equivalent, normal and third invariant stresses; case of condensed microvoids

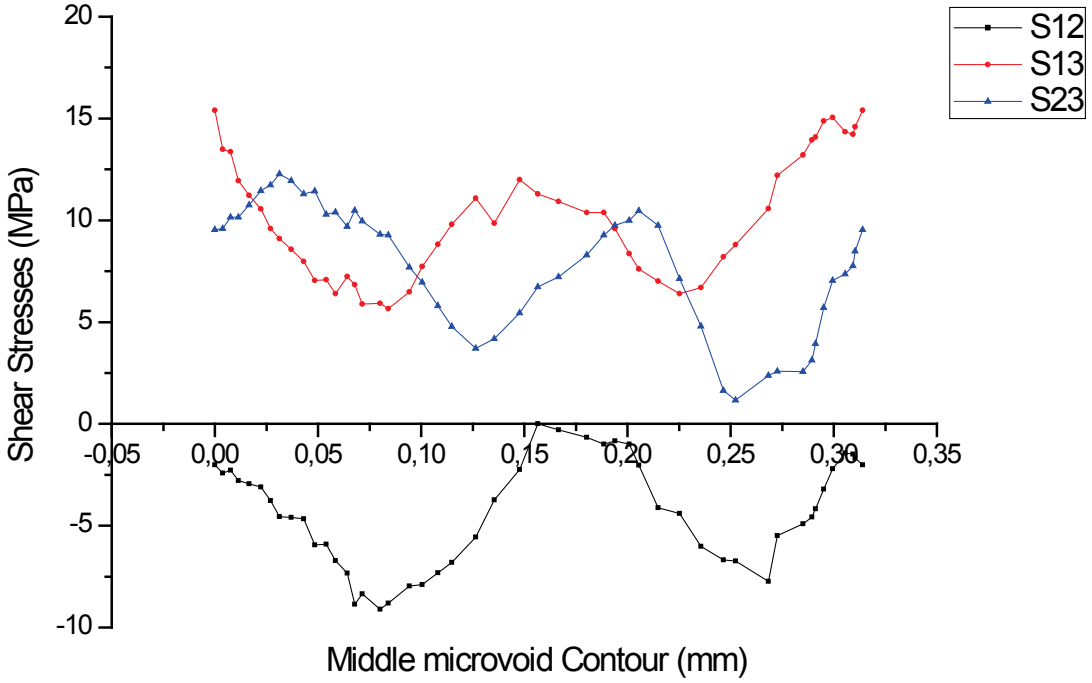

Fig. 5c -Variation of shear stresses; case of condensed microvoids

The variations of deferent stresses around the middle microvoid are illustrated in Figs. 5b&c. The equivalent stress brushes the 40 MPa level, which is the shear rupture limit. Such a level can damage the material and consequently leading to the loosening of the assembly. This zone is under the highest compressive stresses of σ_{33} compared to σ_{11} and σ_{22}. The normal stress σ_{33} also exceeded the tensile rupture limit of PMMA but with an opposite sign. The shear stresses τ_{12} and τ_{13} have the same appearance but two different levels. The highest level is that of τ_{13} but not causing damage. Shear stress τ_{12} is intensively induced in the structure.

3.2.3 Microvoids aligned in the right of the free side of the cement

The stress cartography shows that the level of the equivalent stress induce in the bone cement with microvoids aligned in the right (Fig. 6a) is almost similar to these in the left (Fig. 6a) with a difference of 0.75MPa.

The obtained results exposed in Figs. 6b and 6c. All the stresses have a similar appearance compared to the Fig. 6b and 6c with a minor difference. In other words, the two distributions have practically the same effect on the mechanical behaviour of the material.

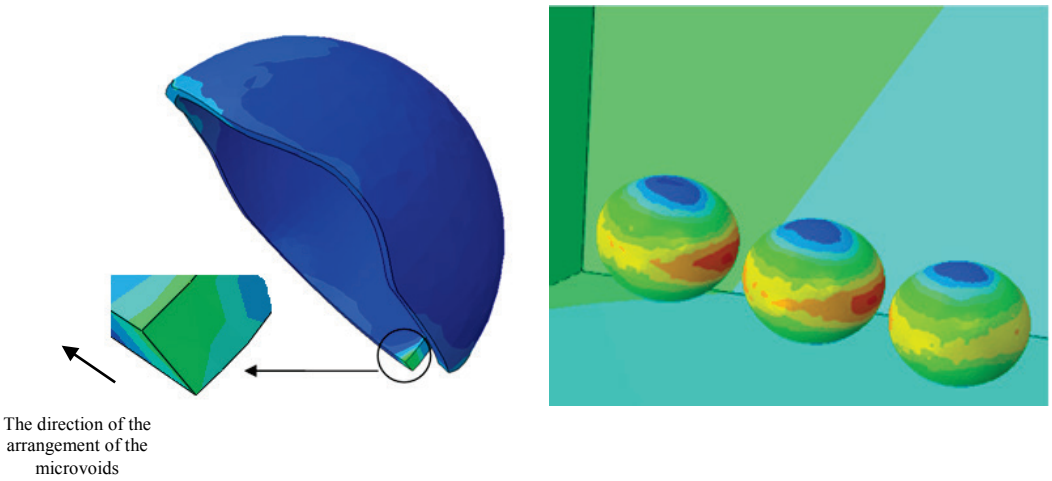

Fig. 6a -Distribution of the equivalent stress of Von Mises; case of aligned microvoids in the right

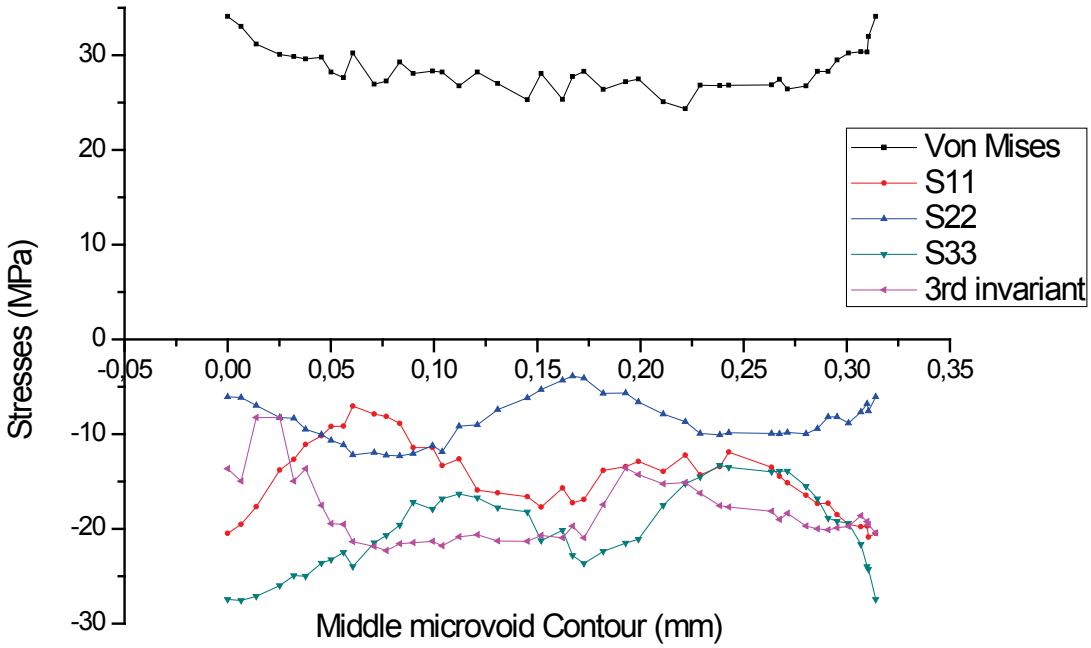

Fig. 6b -Variation of the equivalent, normal and third invariant stresses; case of aligned microvoids in the right

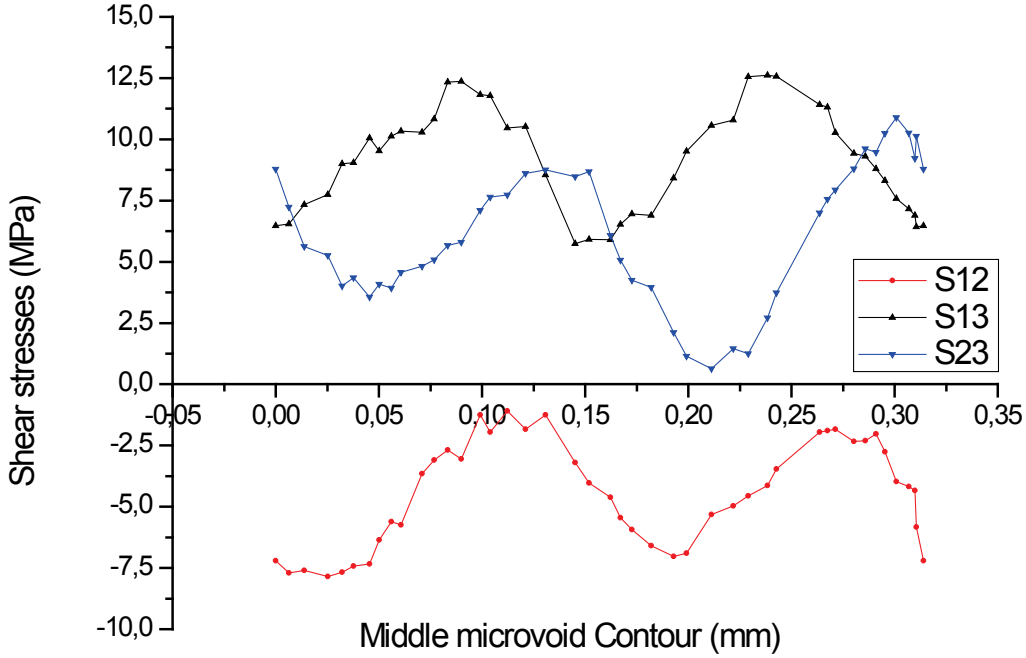

Fig. 6c - Variation of shear stresses; case of aligned microvoids in the right

3.2.4 Microvoids aligned along the thickness in the corner of the free side of the cement

In Fig. 7a are shown the level and distribution of equivalent stress induced in the surgical cement. They are concentrated around the microvoids aligned along the thickness at the free side (free corner) and from the cement/bone to cement/cup interfaces. This distribution of defects in this section (thickness) compared to other arrangement put the structure in strongest stress.

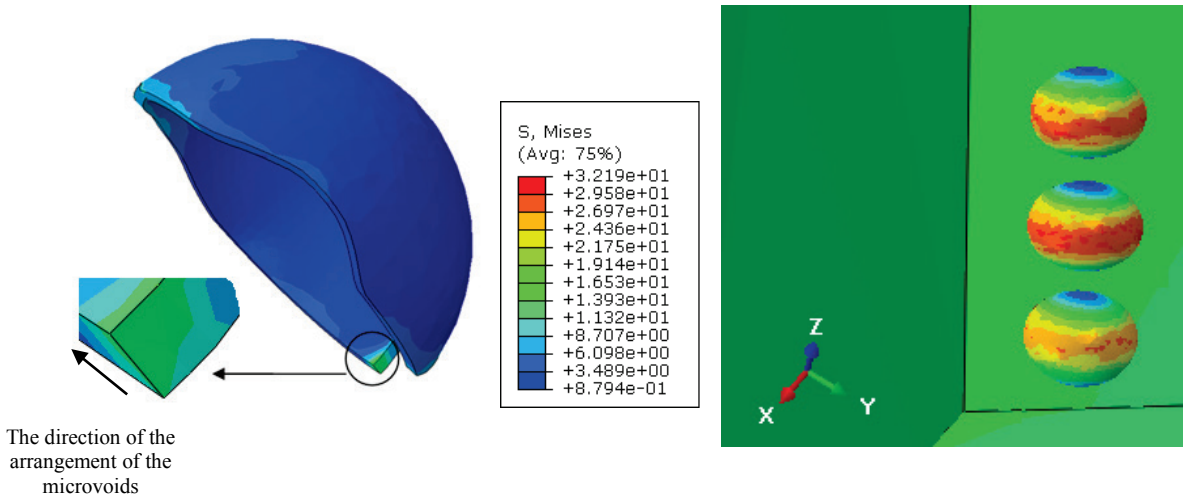

Fig. 7a - Distribution of the equivalent stress of Von Mises; case of aligned microvoids along the thickness of the cement

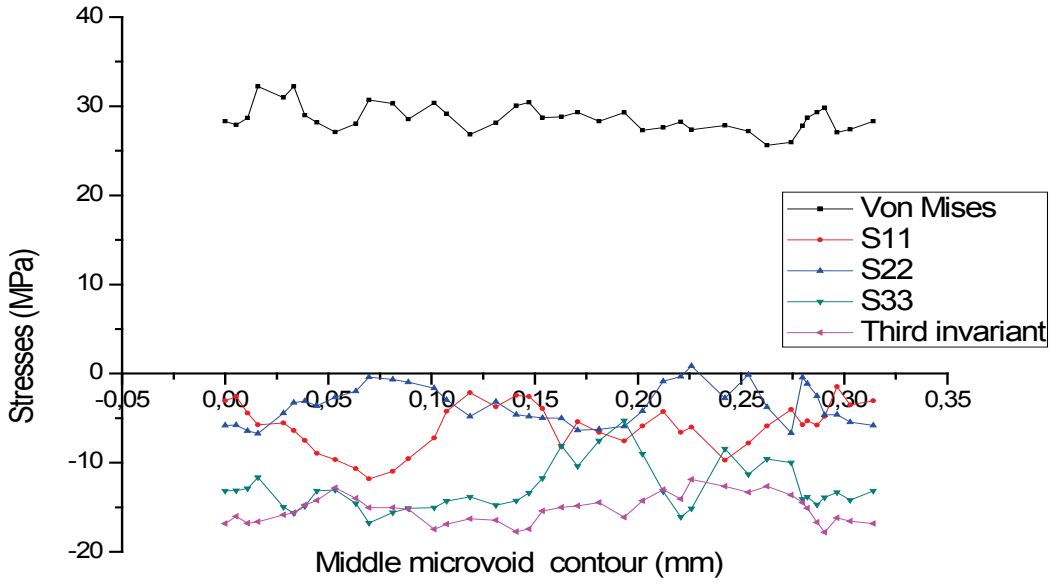

Fig. 7b- Variation of the normal and third invariant stresses; case of aligned microvoids along the thickness of the cement

The maximum Von Mises stresses are located around the middle microvoid (Fig. 7b). The highest amplitudes is much upper than the ultimate tensile stress. The peak of compression stress σ_{33} is lower than the ultimate compression stress. The variation of the other normal stresses σ_{11} and σ_{22} is relatively very weak.

The strongest tangential stresses on the (oxz) plane (τ_{13}) (Fig. 7c), the shear stresses τ_{23} and τ_{12} have almost the same appearance but lower amplitude. Away from this area, these stresses have a low intensity.

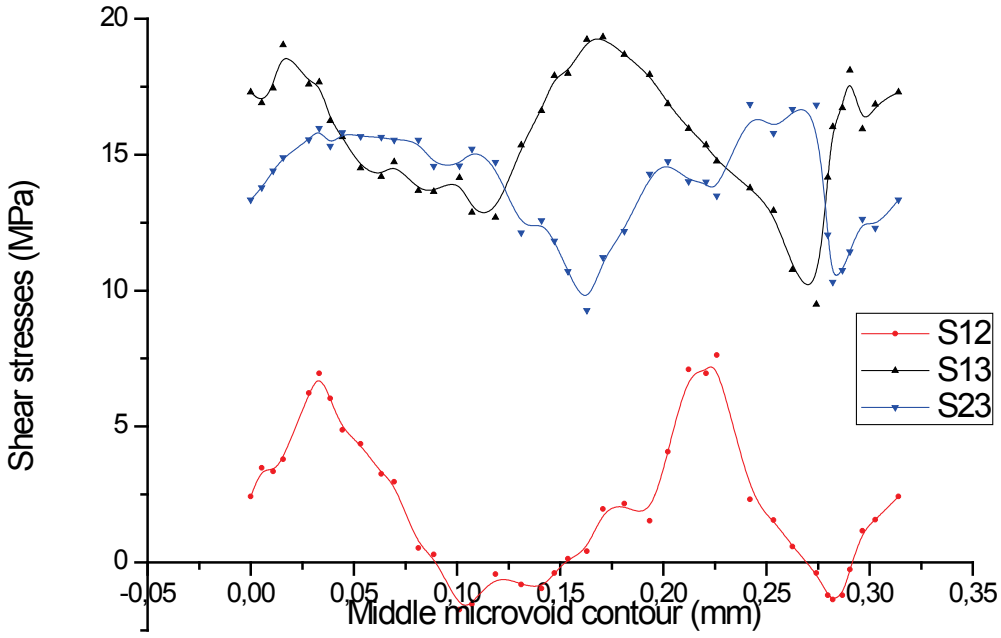

Fig. 7c - Variation of the equivalent and shear stresses; case of aligned microvoids along the thickness of the cement

Comparative study

The comparative analysis of the results obtained for different distributions of microvoids shows that the Von Mises stresses induced in orthopaedic cement according to the distribution of defects and their localization in the vicinity close of the free side of the cement and at the interface cement/bone.

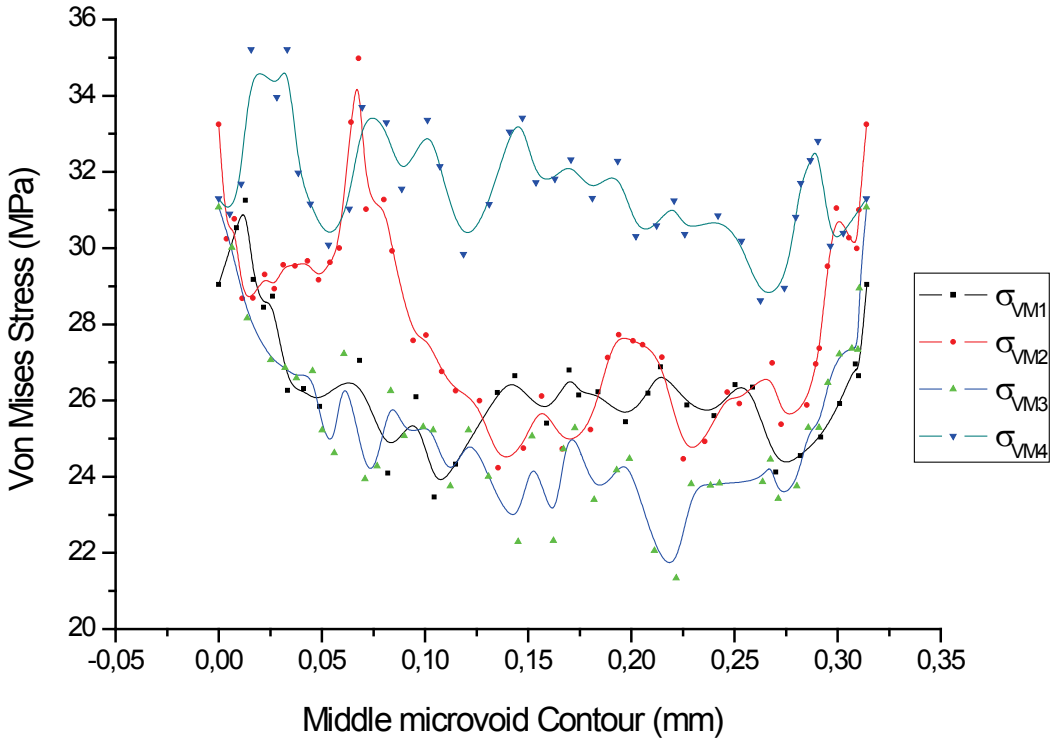

Fig. 8- Comparison of variation of the equivalent stress for all cases

Indeed, the highest stress was observed in Figs. 5 and 7 (condensed and aligned microvoids along the thickness of the cement), these distributions have generated high intensity share stresses around the middle microvoid compared to the other distributions. This amplitude exceeds the ultimate tensile rupture of the orthopaedic cement that can lead to the risk of loosening of the prosthesis.

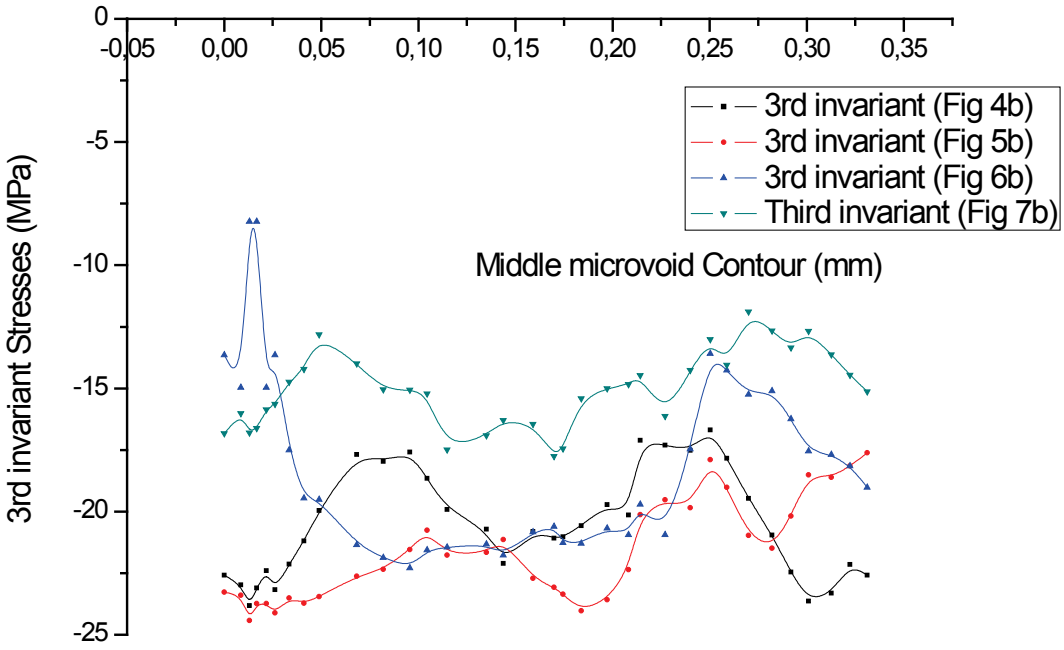

Fig. 9- Comparison of variation of the 3rd invariant stress for all cases

The third invariant differs from one arrangement to the other of microvoids. The most striking value in absolute value is that of Figure 5b. This means that this arrangement is the most dangerous for cement and leads to its loosening.

4 Conclusion

We summarize the results and note that the most significant normal stress is σ_{33} in the direction of the vertical axis (oz). Indeed, the force Fz applied in the direction (oz) acting on the femoral head generates an intensive compressive stress σ_{33} around the central microvoid. The normal stresses σ_{11} and σ_{22} are less than σ_{33}. The third invariant around the central microvoid has almost the same appearance but with a different minor in the amplitude variation with the compression stress σ_{33}. On the other hand, the most important shear stresses are in the (oxz) plane and they are practically localized near the free edge of the cement and at the cement / bone interface. The maximum amplitude of the shear stresses is much smaller than the ultimate shear stresses. The rest of the surgical cement is under low stress. In the comparative analysis, the highest stress was observed on condensed and aligned microvoids along the thickness of the cement. This amplitude exceeds the ultimate fracture rupture of the orthopaedic cement that may lead to a risk of loosening of the prosthesis. The amplitude of the third invariant is high in absolute value for the condensed location of microvoids.

REFERENCES

[1]- D. Charef, B. Serier, Effects of dynamic loading on the mechanical behavior of total hip prosthesis, J. Biomech. Sci. Eng. 10(4) (2015). doi:10.1299/jbse.15-00115.

[2]- M.E. Belgherras, B. Serier, L. Zouambi, Elliptic crack behavior emanating from the cement mantle of the total hip prosthesis. Polym. Test. 61 (2017) 441-447. doi:10.1016/j.polymertesting.2017.06.003.

[3]- L. Zouambi, B. Serier, N. Benamara, Effect of cavity-defects interaction on the mechanical behavior of the bone cement. Adv. Materials Res. 1(3) (2014) 181-193. doi:10.12989/amr.2014.3.1.271.

[4]- B. Serier, L. Zouambi, M.M. Bouziane, S. Benbarek, B. Bouiadjra, Simulation of a Crack Emanating from a Microvoid in Cement of a Reconstructed Acetabulum. In: Properties and Characterization of Modern Materials, Advanced Structured Materials 33, Ed. A. Öchsner and H. Altenbach, 2017, pp. 31-42.

[5]- L. Zouambi, B. Serier, H. Fekirini, B. Bouiadjra, Effect of the Cavity-Cavity Interaction on the Stress Amplitude in Orthopedic Cement. J. Biomater. Nanobiotech. 1(4) (2013) 30-36. doi:10.4236/jbnb.2013.41005.

[6]- ABAQUS Ver 9-11, User Guide; 2011. H.K. Sorensen. Abaqus user manual.

[7]- I.R. Spears, M. Pfleiderer, E. Schneider, E. Hille, M.M. Morlock, The effect of interfacial parameters on cup-bone

relative micromotions. A finite element investigation. J. Biomech. 1(34) (2001). doi:10.1016/S0021-9290(00)00112-3.

[8]- J. Tong, K.Y. Wong, Mixed mode fracture in reconstructed acetabulum. In : Proceedings of the 11th International Conference on Fracture ICF11, Torino, 2005.

[9]- S. Benbarek, B. Bouiadjra, T. Achour, M. Belhouari, B. Serier, Finite element analysis of the behaviour of crack emanating from microvoid in cement of reconstructed acetabulum. Mater. Sci. Eng. A-Struct. 457(1-2) (2007) 385-391. doi:10.1016/j.msea.2006.12.087

[10]- D. Merckx, Les ciments orthopédiques dans Conception des prothèses articulaires, Biomécanique et biomatériaux. Cahiers d'enseignement de la SOFCOT. Expansion scientifique française, 1993, pp. 67-76.

[11]- P.N. Nocollela, B.H. Thacker, H. Katoozian, D.T. Davy, The effect of interfacial parameters on cup-bone relative micromotions. A finite element investigation. In: Proceeding of Bioengineerion Conférence, LIT, 2001 (50), pp. 427-428.

[12]- G. Bergmann, G. Deuretzbacher, M. Heller, F. Graichen, A. Rohlmann, J Strauss, G.N. Duda. Hip contact forces and gait patterns from routine activities. J. Biomech. 34(7) (2001) 859-871. doi:10.1016/S0021-9290(01)00040-9.

[13]- A. Kusaba, Y. Kuroki, S. Kondo, I. Hirose, Y. Ito, N. Hemmi, Y. Shirasaki, T. Tateishi, J. Scholz, Friction of Retrieved Hip Prostheses, Orthopaedic Proceedings, vol. 86-B, Supp IV, 2018.

[14]- R.B. Pęcherski, P. Szeptyński, M. Nowak, An Extension Of Burzyński Hypothesis Of Material Effort Accounting For The Third Invariant Of Stress Tensor. Arch. Metall. Mater. 56(2) (2011) 503-508. doi:10.2478/v10172-011-0054-4.

[15]- D.S. SIMULIA, Abaqus Theory, Guide, http://abaqus.software.polimi.it/v6.14/books/stm/default.htm.